HHS Public Access

Author manuscript

Brain Res. Author manuscript; available in PMC 2021 July 15.

Published in final edited form as:

Brain Res. 2020 July 15; 1739: 146832. doi:10.1016/j.brainres.2020.146832.

Comparison of High-Dose Intracisterna Magna and Lumbar Puncture Intrathecal Delivery of AAV9 in Mice to Treat Neuropathies

Rachel M. Bailey[1,2,3], **Alejandra Rozenberg**[1], **Steven J. Gray**[1,2,4,5,6]

[1]Gene Therapy Center, University of North Carolina at Chapel Hill;

[2]Department of Pediatrics, University of Texas Southwestern Medical Center, Dallas, TX;

[3]Center for Alzheimer's and Neurodegenerative Diseases, University of Texas Southwestern Medical Center, Dallas, TX

[4]Department of Ophthalmology, University of North Carolina School of Medicine, Chapel Hill, NC;

[5]Department of Molecular Biology, University of Texas Southwestern Medical Center, Dallas, TX;

[6]Department of Neurology and Neurotherapeutics, University of Texas Southwestern Medical Center, Dallas, TX

Abstract

Gene therapy clinical trials for neurological disorders are ongoing using intrathecal injection of adeno-associated virus (AAV) vector directly into the cerebral spinal fluid. Preliminary findings from these trials and results from extensive animal studies provides compelling data supporting the safety and benefit of intrathecal delivery of AAV vectors for inherited neurological disorders. Intrathecal delivery can be achieved by a lumbar puncture (LP) or intracisterna magna (ICM) injection, although ICM is not commonly used in clinical practice due to increased procedural risk. Few studies directly compared these delivery methods and there are limited reports on transduction of the PNS. To further test the utility of ICM or LP delivery for neuropathies, we performed a head to head comparison of AAV serotype 9 (AAV9) vectors expressing GFP injected into the cisterna magna or lumbar subarachnoid space in mice. We report that an intrathecal gene delivery of AAV9 in mice leads to stable transduction of neurons and glia in the brain and spinal cord and has a widespread distribution that includes components of the PNS. Vector expression was notably higher in select brain and PNS regions following ICM injection, while higher amounts of vector was found in the lower spinal cord and peripheral organs following LP injection. These

Correspondence can be addressed to: Rachel Bailey, University of Texas Southwestern Medical Center, 5323 Harry Hines Blvd, Dallas, TX 75390-8593, T: 214-648-8510, Rachel.Bailey@UTSouthwestern.edu Or Steven Gray, Steven.gray@UTSouthwestern.edu.

Disclosures

S.J.G. declares a conflict of interest with Asklepios Biopharma, from which he has received patent royalties for IP that are not used in this study.

findings support that intrathecal AAV9 delivery is a translationally relevant delivery method for inherited neuropathies.

Keywords

Adeno-associated virus; Intrathecal; Intracisterna Magna; Lumbar Puncture; Neuropathy; Peripheral Nervous System

1. Introduction

Inherited neuropathies result from genetic defects in a variety of genes important for neuronal function. Recessively inherited disorders cause loss of function in a variety of genes expressed in neurons, supportive glial cells or both. Therapeutic correction can be achieved through gene replacement therapy and various techniques have been developed for gene delivery. Adeno-associated virus (AAV) has emerged as one of the safest and most commonly used vectors for gene delivery due to their ability to infect non-dividing cells, high transduction efficiency, long-lasting expression from a single dose, and a relatively low host immune response (1). AAV9 has emerged as one of the most frequently used serotypes for neurological disorders due to its ability to cross the blood-brain barrier and from its high transduction of neural tissue (2). While intravenous injection of AAV9 results in wide-spread delivery of vector to the CNS and systemic organs, caveats include a larger viral vector dose for treatment and an increased contact of AAV vectors with neutralization antibodies in the blood before they can reach the CNS (3–5). Delivery of AAV vectors into the cerebrospinal fluid (CSF) can achieve gene transfer to cells throughout the brain and spinal cord, potentially making many inherited neurological diseases tractable gene therapy targets.

A lumbar puncture (LP) is the standard approach to do an intrathecal injection in humans. However, this route can be technically challenging in some animal models due to anatomical differences between humans and other species. Based on work in mice, rats, pigs, and nonhuman primates, the LP intrathecal approach was demonstrated to achieve efficient gene transfer to motor and sensory neurons in the central nervous system (CNS) and dorsal root ganglia (DRG) (5–12). In addition to the initial use of the LP route to deliver AAV9 in a clinical trial for Giant Axonal Neuropathy (GAN) in 2015 (clinicaltrials.gov identifier NCT02362438), this approach is being used in ongoing clinical trials for Spinal Muscular Atrophy, CLN3 Batten Disease, and CLN6 Batten Disease (clinicaltrials.gov identifiers NCT03381729, NCT03770572, and NCT02725580) (13, 14). Together these trials provide compelling data regarding the safety and potential benefit of CSF delivery of AAV9 vectors for treating inherited neuronal disorders and axonopathies.

Vector delivery into the CSF can also be achieved by intracisterna magna (ICM) injection, although this procedure is not commonly used in clinical practice. Recent studies in animals show that ICM vector delivery is a safe and effective method for AAV9 delivery and may target the brain to a higher extent than LP delivery (15–18); however, studies directly comparing ICM and LP delivery methods are generally limited to the CNS and results between groups may vary based on the animal species, vector design and dose used. To advance our knowledge of using these two delivery methods for treating neuropathies, we

performed a head to head comparison of LP and ICM delivered AAV9 vector in mice. This study expands our previous findings in non-human primates (8) and work by others by using a 10X higher vector dose in mice and reporting a detailed analysis of biodistribution to the CNS, PNS and ANS. Wild-type mice were injected with a high dose of self-complementary AAV9/GFP in age, strain and sex-matched mice to enable direct comparison of vector distribution and expression following LP or ICM delivery. Overall, we found in mice that intrathecal delivery of a high-dose of AAV9 by either route results in efficient CNS transduction and that gene transfer of the peripheral nervous system is also achieved to a lesser extent. Vector expression was notably higher in select brain and PNS regions following ICM injection, while higher amounts of vector was found in the thoracic and lumbar spinal cord regions and overall in systemic organs following LP injection.

2. Results

2.1 Study Design.

In this study, 6 to 8 week old C57BL/6 female mice received an intrathecal injection into the cisterna magna (ICM) or lumbar subarachnoid space (LP) with an AAV9 vector packaging a self-complementary (19) GFP transgene controlled by the CBh promoter (20). The ubiquitous CBh promoter will express in both neurons and astrocytes, in addition to other cell types. By both routes, we evaluated a high intrathecal dose of 4.15×10^{11} viral genomes (vg) per mouse and compared to untreated littermates. Tissues were collected 4 weeks post-injection and either frozen for vector biodistribution (n=5 per injection group; n=2 for untreated group) or fixed for immunohistochemical (IHC) analysis of transgene expression (n=5 per injection group; n=4 for untreated group).

2.2 Vector Biodistribution.

We quantified vector genomes in DNA extracted from CNS, PNS and systemic tissues. Averages per injection group are shown in Figure 1. We detected AAV vector genomes in all tissues analyzed in all vector-treated animals. Vector was not detected in tissues from untreated mice that were analyzed in parallel (data not shown). In the brain, AAV9/GFP vector transduction was significantly higher in the cerebellum and hindbrain (pons and medulla) following ICM injection as compared to LP injection. All other brain regions had similar vector levels. In the spinal cord, vector was significantly higher in the lumbar and thoracic cords from LP delivery as compared to ICM delivery. Likewise, LP injected mice had significantly higher vector in lumbar DRG than ICM injected mice. Vector was detected at low levels in both sciatic and median nerves from both delivery routes. Overall, the biodistribution results show that in the CNS, vector copies are highest closest to site of injection, which is hindbrain and cerebellum for ICM and lumbar spinal cord for LP.

The vector was distributed to the peripheral organs, especially the liver, with vgs around 3 copies per mouse genome following ICM injection and around 5 copies per mouse genome following LP injection. Vector copies were higher in most of the peripheral tissues tested following LP delivery with vgs in the spleen being significantly increased as compared to ICM delivery. By both methods, a significant amount of vector escapes to the peripheral

circulation as evident by high liver and spleen distribution. In support of this, low levels of AAV vectors were also detected throughout the gastrointestinal tissues.

2.3 Central Nervous System Expression.

For analysis of overall vector transduction in the CNS, formalin-fixed brain and spinal cords from intrathecal vector injected and untreated mice were analyzed for GFP expression in free-floating sections. Although native GFP fluorescence was visible in unstained brain and spinal sections (data not shown), we've previously shown that GFP IHC combined with a Vectastain ABC secondary detection kit provides greater sensitivity with minimal background (5). Transduction of all brain areas and spinal cord was evident by both intrathecal delivery methods (Figures 2 and 3). In agreement with the biodistribution results, GFP transduction was greater in the cerebellum and hindbrain of ICM injected mice as compared to LP injected mice. Overall GFP expression shows that ICM AAV9 transduction was a gradient with the highest levels of expression in the hindbrain that decreases towards the forebrain (Figure 2A). As such, deeper brain structures such as the thalamus and striatum were similarly transduced by both ICM and LP delivery at this high dose (Figure 3). In the spinal cord, GFP transduction was very high at all levels by both delivery methods and there was not a noticeable difference between them (Figure 2B), contrary to what would be expected based on the biodistribution results. This difference may be due to saturation of GFP signal by this detection method.

Morphologically, GFP positive cells are a mix of neurons and glia throughout the brain (Figure 3). In certain regions, such as the hippocampus, cortex and cerebellum, staining shows higher transduction of neurons than glia by both delivery methods. Hindbrain regions (midbrain, pons and medulla) indicate potentially greater glial transduction by LP delivery and cannot be ascertained in ICM injected animals due to the saturation of GFP expression. To further analyze cellular transduction by intrathecal AAV9 vectors, we performed fluorescent co-labeling studies. Thin brain sections were stained with GFP antibody and either NeuN (neurons) or GFAP (astrocytes) and showed that AAV9 efficiently transduced a mix of mostly neurons and astrocytes by both delivery methods; representative images from an area with moderate transduction (cortex) and high transduction (medulla) are shown in Figure 4. No co-labelling was seen with Iba1 (microglia) (data not shown). Brain regions with very high GFP transduction, such as the medulla in ICM injected mice, showed an increased number of GFAP positive cells (Figure 4B) and Iba1 positive cells (data not shown) as compared to LP injected or untreated animals. GFAP is known to be upregulated in reactive astrocytes and Iba1 in active microglia, indicating and astrogliosis response to high, localized AAV9/GFP transduction in the brain.

2.4 Peripheral Nervous System Expression.

For many inherited neurological disorders it is critical to correct cells located within the brain and spinal cord; however, for recessive neuropathies, such as GAN, targeting of peripheral and autonomic tissues is also critical for disease treatment (21). We and others have shown that intrathecal delivery of AAV9 vectors very efficiently target DRGs and components of the autonomic nervous system and enteric nervous systems (6, 8, 22). To visualize nerves and ganglia of the autonomic and enteric nervous systems, we performed

GFP IHC on paraffin embedded sections (Figure 5). As expected, both ICM and LP injection of AAV9 resulted in near complete transduction of lumbar dorsal root ganglia. There was not a notable difference in delivery route and transduction efficiency, but this may reflect having reached near-saturating levels. Intrathecal delivery of AAV9 resulted in GFP expression in longitudinal sections of sciatic nerve. When we assessed components of the autonomic nervous system, we found that paravertebral sympathetic chain ganglia were transduced by both injection routes, with ICM delivery having greater transduction than LP delivery, particularly in the cervical region. In line with previous studies, we found that enteric neurons in the myenteric plexus and submucosal plexus within the intestines were transduced following intrathecal delivery of AAV9. Overall, these findings support that intrathecal AAV9 delivery by ICM or LP delivery can transduce tissues and cells relevant for treating many inherited neuropathies.

3. Discussion

Inherited neuropathies are a heterogeneous group of disorders in both causes and clinical presentations. These disorders can be broadly characterized by involvement of only the PNS, by involvement of both the CNS and PNS or as a neuropathy with multiorgan involvement affecting non-neurological organs (23). Having a gene transfer strategy capable of achieving high levels of transduction throughout the CNS, PNS and organs could greatly expand the applications of gene therapy in inherited neuropathies. There are multiple methods to deliver therapeutic genes and here we focus on the use of AAV9. AAV vectors are small with a limited packaging capability (~4.7 kb), which may preclude packaging of large genes or gene editing systems such as CRISPR/CAS9 into a single vector. Further, the self-complementary AAV used in this study would limit the genome packaging capacity to ~2.2 kb of foreign DNA, and if traditional single-stranded AAV vectors were used one would expect lower transduction efficiency. For diseases where AAV vectors are suitable, AAV9 has emerged as the gold standard to target the nervous system given its desirable safety profile, strong neuronal tropism and clinical success. To target AAV9 to the brain and spinal cord a number of preclinical and clinical trials use intracisternal and lumbar subarachnoid injections. To further assess the utility of these methods for targeting components of the CNS, PNS and ANS, we performed a direct comparison of ICM and LP delivery of an AAV9 reporter vector. In agreement with previous studies, we found that intrathecal AAV9 delivery is an attractive strategy due to its direct access to the CSF, which enabled high transduction of nervous tissues and escaped to the periphery to transduce multiple organs. Importantly, we show that vector distribution and expression is highest in the CNS closest to the site of injection and report an expanded distribution profile of the whole body and nervous system, including components of the CNS, PNS and ANS that are critical to a number of neuropathies.

In mice we found that the level of CSF access had a significant effect on vector distribution in the CNS. This agrees with the a head to head comparison study of ICM and LP delivery in cynomolgus macaques (15), but where they reported that intercisterna delivery of AAV9 vector was more efficient than lumbar puncture delivery for gene transfer to both the brain and spinal cord, we found this to only be true for the brain. We also found that vector transduction in deep brain regions, such as the striatum and thalamus, was equivalent

between intracisterna and lumbar subarachnoid injections in mice. Differential results in our study and the Hinderer *et al* study could be in part from 1) inherent differences in vector transduction between primates and rodents, 2) lower animal numbers in primate studies; 3) use of a less-efficient single-stranded vector compared to our self-complementary vector (24); 4) differences in dose resulting in reduced spread; or 5) Assessing native GFP which may underestimate GFP levels in cells with low expression. Further, anatomical differences, particularly at the lumbar cistern, can create technical challenges that will vary considerably across species. In a recent study by Ohno *et al*, 2/3 of NHPs administered AAV9 showed extensive leakage of the injection solution out of the CSF following an LP while all of the NHPs receiving an ICM injection retained the injection solution within the CSF (25). In the Ohno study where the infusion was monitored by MRI, the poor biodistribution of AAV9 following an LP could be explained by this technical caveat, but this type of injection fidelity monitoring is rarely done in preclinical biodistribution studies. Regardless of differences, results from both studies suggest that the site of injection can be leveraged to fine-tune expression in the CNS as essential for a given disease.

In this study we maximized potential vector spread and detection by using a self-complementary vector with the strong, ubiquitous CBh promoter at the highest feasible dose as delineated by the vector titer and volume allowed for LP injections. Self-complementary vectors have higher transduction efficiency than single stranded AAV vectors (5, 19) and the CBh promoter provides robust expression of our reporter protein (20), allowing us to readily track those cells infected by AAV9 from each delivery method. While the design of the vector in this study facilitates high transgene expression in a maximal number of cells, promoter selection for therapeutic vectors should take into account the packaging limitation of AAV vectors, desired transgene expression level and whether expression should be cell-type restricted given the precise genetic mechanisms underlying a given disorder. A high intrathecal dose of 4.15×10^{11} vg may have contributed to the vector distribution gradient we found from the site of injection by both routes as well as to the wide-spread brain expression of scAAV9/GFP following LP delivery. Notably, we saw increased astrogliosis in the hindbrain following ICM injection that was absent in areas with lower transduction, such as the cortex and in LP injected or untreated mice. In a study by Samaranch *et al*, they report a similar finding in cynomolgus macaques that received an ICM injection of AAV9/GFP and not in animals that received an AAV9/hAADC vector (26). The Samaranch study showed that AAV9-mediated expression of a non-self protein (GFP) in the brain of non-human primates triggers widespread neuroinflammation. This could explain our findings in AAV9/GFP ICM injected mice, but raises additional questions as to the dependency on local dose or route of injection as we did not see a similar response in mice LP injected with the same dose of AAV9/GFP. So while high-transduction AAV9 studies can be very informative, care should be given to assess possible immune responses that could confound results.

A translationally-relevant gene therapy approach for inherited neuropathies must take into account targeting the essential cell type(s) underlying the major pathophysiology of that disorder. For example, Charcot-Marie-Tooth disease (CMT) is a collection of inherited motor and sensory neuropathies where mutations in over eighty genes can lead to CMT (27). Individual mutations underlie a pathophysiology that can be attributed to loss of peripheral motor and sensory axon function through demyelination, axon degeneration, or a

combination of these mechanisms (28). For axonopathies and mixed demylenating-axonopathies, therapeutic benefit may be achieved through rescue of neurons even if there is not efficient transduction of Schwann cells. For example, a recent study by Morelli et al. investigated LP intrathecal delivery of a self-complementary AAV9 vector carrying a mutant-allele specific artificial microRNA expression cassette in mouse models of the axonopathy CMT disease type 2D (29). Even after symptom onset, LP delivery of AAV9 gene therapy provided a significant benefit in preventing neuropathy as evidenced by increased grip strength, neural conduction velocities and neural muscular junction innervation and a reduction in axon loss. While LP intrathecal scAAV9 gene therapy prevented neuropathy in an axonopathy CMT disease type, this delivery approach may have limited benefits for purely demyelinated CMT disorders.

Currently, it is unclear if Schwann cells are transduced by intrathecal-delivered AAV9, but results from this study suggests that it may, at least to a small extent. Our biodistribution studies detected a low amount of vector DNA in peripheral nerves and the nerve samples we analyzed contains motor and sensory neuron axons ensheathed by Schwann Cells and surrounding endonerium and perineurium cells. We anticipate that vector DNA is present in the nucleus of a cell, where it was delivered during AAV trafficking and uncoating, suggesting that AAV9 transduced a low number of Schwann cells and/or endonerium and perinerium cells. IHC analysis of sciatic nerves showed positive vector expression, however, it is unclear if GFP expression is localized to axons, Schwann cells, epineurium/perineurium or a combination. Additional studies using co-labeling and/or teased fiber preps would be ideal for determining if AAV9 transduces Schwann cells following intrathecal delivery. While AAV9 transduction of Schwann cells remains unknown, a therapeutic benefit might still be achievable for diseases with Schwann cell defects. For example, in our GAN preclinical studies, we found that GAN KO mouse peripheral nerve showed axonal loss preferentially involving small diameter myelinated fibers and unmyelinated fibers with severe and pronounced intermediate filament accumulation within axons and Schwann cell cytoplasm as part of the disease pathophysiology (6). GAN KO mice were treated with a single LP injection of an AAV9/GAN vector and we found that treated GAN KO mice showed relatively well-preserved unmyelinated fibers and large diameter myelinated fibers with overall increased profiles of normal appearing Schwann cells. These results suggest that for some inherited neuropathies, therapeutic benefits in Schwann cells can be achieved by predominantly targeting and treating neurons that they associate with.

The present results suggest that both intracisternal and lumbar subarachnoid injections of AAV9 are suitable for diffuse and global transduction of the CNS and DRG and for limited transduction of peripheral nerves and autonomic nervous tissue, including sympathetic and enteric neurons. In mice, both ICM and LP administration routes transduced both glia and neurons including motor, sensory, autonomic and enteric neurons. For inherited neuropathies, ICM delivery could be promising for disorders affecting hindbrain areas such as the cerebellum and brainstem whereas LP delivery may be of greater use for gene therapies targeted to the spinal cord. Overall, intrathecal delivery of AAV9 represents a tractable gene delivery method for many inherited neuropathies and neurological disorders.

4. Experimental Procedures

4.1 Experimental animals.

Animal studies were performed in accordance with the Guide for the Care and Use of Laboratory Animals (DHHS Publication no. (NIH) 85-23) and approved by the University of North Carolina at Chapel Hill Institutional Animal Care and Use Committee. C57BL/6 breeders were obtained from Jackson laboratories and maintained at UNC Chapel Hill. Female mice were used in these studies and provided food and water ad libitum. Mice were randomized into treatment groups (ICM, n=10; LP, n=10; or untreated, n=6) and injected between 6 and 8 weeks of age.

4.2 Virus.

A reporter vector was used in these studies where gene expression cassette ended eGFP under the control of the CBh promoter (20) and with a SV40 polyadenylation signal. Self-complementary AAV vector was produced using methods developed by the University of North Carolina (UNC) Vector Core facility, as described (30). The purified AAV was dialyzed in PBS supplemented with 5% D-Sorbitol and an additional 212 mM NaCl (350 mM NaCl total). Vector was titered by quantitative PCR (31) and confirmed by polyacrylamide gel electrophoresis and silver stain. The same lot of vector was used in all studies.

4.3 Intrathecal injections.

LP: AAV9 vector was injected with a maximal feasible dose at a total volume of 5 μL per animal. The injection was performed by lumbar puncture into the subarachnoid space of the lumbar thecal sac: the animal was conscious and held in position for a free-hand injection into the posterior midline site at ~ lumbar 4/5 level identified (below the conus of the spinal cord), as described (31).

ICM: AAV9 vector was diluted in the vehicle and the total volume injected for each animal was 10 μL. Vehicle was 350mM PBS with 5% D-sorbitol. ICM injections were performed as a bolus injection into the cisterna magna as previously described (18). The vector dose used for all injections was 4.15×10^{11} vg/mouse.

4.4 Vector biodistribution.

Mice were deeply anesthetized with an overdose of avertin (0.04 mL/g of a 1.25 % solution) and perfused with PBS containing 1 μg/mL heparin. Tissues were quickly dissected, immediately frozen on dry-ice and stored at −80 °C. Brain was sub-dissected into the following regions: cerebellum, hindbrain (pons and medulla), midbrain to striatum (includes thalamus, hypothalamus, amygdala, etc.), hippocampus, cortex, olfactory bulbs and optic chiasm. Spinal cord was divided into cortical, thoracic and lumbar regions and dorsal root ganglia from each region was collected. Sciatic nerves and median nerves were isolated from legs and arms, respectively. The entire gut was removed, rinsed briefly in PBS and caecum, duodenum and rectum regions isolated. Other tissues collected included salivary glands, esophagus, pancreas, liver, heart, lung, spleen, kidney muscle and ovaries (gonads). For vector biodistribution, DNA was extracted and quantified by qPCR as previously

described (5). Data is reported as the number of double-stranded GFP DNA molecules per 2 double-stranded copies of the mouse LaminB2 locus, which is the number of vector DNA copies per diploid mouse genome. Biodistribution data from one ICM-injected mouse and one LP injected mouse were excluded due to extremely high vector content in the hindbrain (19.9 vg/mouse genome) and lumbar cord (11.5 vg/mouse genome), suggesting the CNS tissue was nicked by the needle during delivery and biodistribution results do not accurately reflect spread by each route.

4.5 Immunohistochemistry.

Mice were deeply anesthetized with an overdose of avertin (0.04 mL/g of a 1.25 % solution) and perfused with PBS containing 1 μg/mL heparin and then perfused with 10% formalin. For overall GFP expression in the central nervous system, brains and spinal cords were drop-fixed in 10% formalin for 48 hours before being moved to PBS. Tissues were then vibratome sectioned into 40 μm coronal slices using a Leica Vibratome (VT 1000S; Leica Biosystems Inc., Buffalo Grove, IL) and stored in PBS at 4°C. Every 5th section from the whole brain and spinal cords of each animal was stained free-floating as previously described (32). Primary antibody was anti-GFP (1:2000) (Millipore, 3080) and biotinylated anti-rabbit secondary antibody (1:2000) (Vector Laboratories, Burlingame, CA).

For analysis of GFP expression in the peripheral nervous system, tissues were drop-fixed, paraffin embedded and microtome sectioned as previously described (6, 21). 5 μm sections were stained with the primary antibody anti-GFP (1:1000) (Aves, GFP-1020) and biotinylated anti-chicken secondary antibody (1:200) and hematoxylin counterstained for light microscopy as previously described (21). Immunostained sections were digitally imaged in a bright field (20X objective) using a ScanScope XT instrument (Leica Biosystems Inc., Buffalo Grove, IL) by the UNC Translational Pathology Laboratory. Digital images were obtained using Leica eSlide Manager (centralized image storage and data management software) and analyzed using Aperio ImageScope software.

4.6 Immunofluorescence.

For cell-type specific studies, 5 μm sections were deparafinized following standard techniques. For NeuN staining, sections were then immersed in antigen retrieval solution (AUS, Vector H-3300) and incubated in a pressure cooker under high pressure for 10 minutes. Sections were then cooled at room temperature for 20–30 minutes before being washed with dH_2O. Slides were then washed 3 times with PBS prior to blocking for 1 hour at room temperature in 10% goat serum (in PBS, 0.1% Tween 20). Tissue sections were then incubated with primary antibodies diluted in 2% goat serum (in PBS, 0.1% Tween 20) overnight at 4°C; anti-GFP (1:750) (Aves, GFP-1020) and anti-NeuN (1:1000)(Millipore, MAB377). Sections were washed 3 times with PBS and incubated with secondary antibodies diluted in 2% goat serum (in PBS, 0.1% Tween 20) for 1 hour at room temperature; 594-alexa Fluor goat anti-mouse (1:1000) (Molecular Probes – Life Technologies, A11032) and 488-alexa Fluor goat anti-chicken (1:1000) (Molecular Probes – Life Technologies, A11029). For GFAP staining, antigen retrieval was not used. Following deparafinization, sections were washed 3 times in PBS and then blocked for 1 hour at room temperature in 10% goat serum (in PBS, 0.1% Tween 20). Tissue sections were then incubated with

primary antibodies diluted in 2% goat serum (in PBS, 0.1% Tween 20) overnight at 4°C; anti-GFP (1:750) (Aves, GFP-1020) and anti-GFAP (1:1000) (DAKO 20025481). Sections were washed 3 times with PBS and incubated with secondary antibodies diluted in 2% goat serum (in PBS, 0.1% Tween 20) for 1 hour at room temperature; 594-alexa Fluor goat anti-rabbit (1:1000) (Molecular Probes – Life Technologies, A11037) and 488-alexa Fluor goat anti-chicken (1:1000) (Molecular Probes – Life Technologies, A11029). For all fluorescent staining, sections were then counterstained by incubating with DAPI (1:2000) for 45 minutes at room temperature. Slides were then mounted with Prolong Gold antifade reagent with DPAI (Fisher, P36391). Fluorescent signal was captured using a ScanScope FL (Leica Biosystems) and was scanned at 20X by the UNC Translational Pathology Laboratory. Digital images were obtained and analyzed as described above.

4.7 Data analysis.

An unpaired t-test was used to compare means for biodistribution analysis. For all comparisons, statistical significance was set at $p < 0.05$. Data were graphed using GraphPad Prism software (v. 8.3.0; GraphPad Software).

Acknowledgements

This work was supported by the National Institutes of Health (grants NS 095515 and HD 040127 to R.M.B.; grants NS 087175 and NS 095867 to S.J.G.) and by Hannah's Hope Fund. The authors wish to thank members of the Gray Lab, especially Caleigh Toppins, Violeta Zaric and Alli Hooper for technical support with mouse injections, quantitative PCR analysis and immunohistochemistical analysis, respectively. Microscopy was performed at the UNC Translational Pathology Laboratory, supported, in part, by funding from The UNC TPL is supported in part by grants from NCI (5P30CA016080-42), NIH (U54-CA156733), NIEHS (3P30 EOS010126-17), UCRF and NCBT (2015-IDG-1007).

Abbreviations (non-standard):

AAV	adeno-associated virus
ICM	intracisterna magna
LP	lumbar puncture
GAN	Giant axonal neuropathy
IHC	immunohistochemistry
GFAP	glial fibrillary acidic protein
vg	viral genomes

References

1. Lentz TB, Gray SJ, Samulski RJ. Viral vectors for gene delivery to the central nervous system. Neurobiol Dis. 2012;48(2):179–88. doi: 10.1016/j.nbd.2011.09.014. [PubMed: 22001604]
2. Murlidharan G, Samulski RJ, Asokan A. Biology of adeno-associated viral vectors in the central nervous system. Front Mol Neurosci. 2014;7:76. doi: 10.3389/fnmol.2014.00076. [PubMed: 25285067]
3. Duque S, Joussemet B, Riviere C, Marais T, Dubreil L, Douar AM, Fyfe J, Moullier P, Colle MA, Barkats M. Intravenous administration of self-complementary AAV9 enables transgene delivery to

adult motor neurons. Mol Ther. 2009;17(7):1187–96. doi: 10.1038/mt.2009.71. [PubMed: 19367261]

4. Foust KD, Nurre E, Montgomery CL, Hernandez A, Chan CM, Kaspar BK. Intravascular AAV9 preferentially targets neonatal neurons and adult astrocytes. Nat Biotechnol. 2009;27(1):59–65. Epub 2008/12/23. doi: 10.1038/nbt.1515 nbt.1515 [pii]. [PubMed: 19098898]
5. Gray SJ, Matagne V, Bachaboina L, Yadav S, Ojeda SR, Samulski RJ. Preclinical differences of intravascular AAV9 delivery to neurons and glia: a comparative study of adult mice and nonhuman primates. Mol Ther. 2011;19(6):1058–69. doi: 10.1038/mt.2011.72. [PubMed: 21487395]
6. Bailey RM, Armao D, Nagabhushan Kalburgi S, Gray SJ. Development of Intrathecal AAV9 Gene Therapy for Giant Axonal Neuropathy. Mol Ther Methods Clin Dev. 2018;9:160–71. Epub 2018/05/17. doi: 10.1016/j.omtm.2018.02.005 S2329–0501(18)30017–2 [pii]. [PubMed: 29766026]
7. Federici T, Taub JS, Baum GR, Gray SJ, Grieger JC, Matthews KA, Handy CR, Passini MA, Samulski RJ, Boulis NM. Robust spinal motor neuron transduction following intrathecal delivery of AAV9 in pigs. Gene Ther. 2012;19(8):852–9. Epub 2011/09/16. doi: 10.1038/gt.2011.130 gt2011130 [pii]. [PubMed: 21918551]
8. Gray SJ, Nagabhushan Kalburgi S, McCown TJ, Jude Samulski R. Global CNS gene delivery and evasion of anti-AAV-neutralizing antibodies by intrathecal AAV administration in non-human primates. Gene Ther. 2013;20(4):450–9. doi: 10.1038/gt.2012.101. [PubMed: 23303281]
9. Karumuthil-Melethil S, Marshall MS, Heindel C, Jakubauskas B, Bongarzone ER, Gray SJ. Intrathecal administration of AAV/GALC vectors in 10–11-day-old twitcher mice improves survival and is enhanced by bone marrow transplant. J Neurosci Res. 2016;94(11):1138–51. doi: 10.1002/jnr.23882. [PubMed: 27638599]
10. Samaranch L, Salegio EA, San Sebastian W, Kells AP, Bringas JR, Forsayeth J, Bankiewicz KS. Strong cortical and spinal cord transduction after AAV7 and AAV9 delivery into the cerebrospinal fluid of nonhuman primates. Hum Gene Ther. 2013;24(5):526–32. doi: 10.1089/hum.2013.005. [PubMed: 23517473]
11. Samaranch L, Salegio EA, San Sebastian W, Kells AP, Foust KD, Bringas JR, Lamarre C, Forsayeth J, Kaspar BK, Bankiewicz KS. Adeno-associated virus serotype 9 transduction in the central nervous system of nonhuman primates. Hum Gene Ther. 2012;23(4):382–9. doi: 10.1089/hum.2011.200. [PubMed: 22201473]
12. Meyer K, Ferraiuolo L, Schmelzer L, Braun L, McGovern V, Likhite S, Michels O, Govoni A, Fitzgerald J, Morales P, Foust KD, Mendell JR, Burghes AH, Kaspar BK. Improving Single Injection CSF Delivery of AAV9-mediated Gene Therapy for SMA: A Dose-response Study in Mice and Nonhuman Primates. Mol Ther. 2015;23(3):477–87. Epub 2014/11/02. doi: 10.1038/mt.2014.210 mt2014210 [pii]. [PubMed: 25358252]
13. Simone C, Ramirez A, Bucchia M, Rinchetti P, Rideout H, Papadimitriou D, Re DB, Corti S. Is spinal muscular atrophy a disease of the motor neurons only: pathogenesis and therapeutic implications? Cell Mol Life Sci. 2016;73(5):1003–20. Epub 2015/12/19. doi: 10.1007/s00018-015-2106-9. [PubMed: 26681261]
14. Ostergaard JR. Paroxysmal sympathetic hyperactivity in Juvenile neuronal ceroid lipofuscinosis (Batten disease). Auton Neurosci. 2018;214:15–8. Epub 2018/08/04. doi: 10.1016/j.autneu.2018.07.003. [PubMed: 30072301]
15. Hinderer C, Bell P, Vite CH, Louboutin JP, Grant R, Bote E, Yu H, Pukenas B, Hurst R, Wilson JM. Widespread gene transfer in the central nervous system of cynomolgus macaques following delivery of AAV9 into the cisterna magna. Mol Ther Methods Clin Dev. 2014;1:14051. doi: 10.1038/mtm.2014.51. [PubMed: 26052519]
16. Hordeaux J, Hinderer C, Goode T, Katz N, Buza EL, Bell P, Calcedo R, Richman LK, Wilson JM. Toxicology Study of Intra-Cisterna Magna Adeno-Associated Virus 9 Expressing Human Alpha-L-Iduronidase in Rhesus Macaques. Mol Ther Methods Clin Dev. 2018;10:79–88. Epub 2018/08/04. doi: 10.1016/j.omtm.2018.06.003 S2329–0501(18)30057–3 [pii]. [PubMed: 30073179]
17. Hordeaux J, Hinderer C, Goode T, Buza EL, Bell P, Calcedo R, Richman LK, Wilson JM. Toxicology Study of Intra-Cisterna Magna Adeno-Associated Virus 9 Expressing Iduronate-2-Sulfatase in Rhesus Macaques. Mol Ther Methods Clin Dev. 2018;10:68–78. Epub 2018/08/04. doi: 10.1016/j.omtm.2018.06.004 S2329–0501(18)30058–5 [pii]. [PubMed: 30073178]

18. Sinnett SE, Hector RD, Gadalla KKE, Heindel C, Chen D, Zaric V, Bailey MES, Cobb SR, Gray SJ. Improved MECP2 Gene Therapy Extends the Survival of MeCP2-Null Mice without Apparent Toxicity after Intracisternal Delivery. Mol Ther Methods Clin Dev. 2017;5:106–15. doi: 10.1016/j.omtm.2017.04.006. [PubMed: 28497072]
19. McCarty DM, Fu H, Monahan PE, Toulson CE, Naik P, Samulski RJ. Adeno-associated virus terminal repeat (TR) mutant generates self-complementary vectors to overcome the rate-limiting step to transduction in vivo. Gene Ther. 2003;10(26):2112–8. doi: 10.1038/sj.gt.3302134. [PubMed: 14625565]
20. Gray SJ, Foti SB, Schwartz JW, Bachaboina L, Taylor-Blake B, Coleman J, Ehlers MD, Zylka MJ, McCown TJ, Samulski RJ. Optimizing promoters for recombinant adeno-associated virus-mediated gene expression in the peripheral and central nervous system using self-complementary vectors. Hum Gene Ther. 2011;22(9):1143–53. doi: 10.1089/hum.2010.245. [PubMed: 21476867]
21. Armao D, Bailey RM, Bouldin TW, Kim Y, Gray SJ. Autonomic nervous system involvement in the giant axonal neuropathy (GAN) KO mouse: implications for human disease. Clin Auton Res. 2016;26(4):307–13. doi: 10.1007/s10286-016-0365-7. [PubMed: 27369358]
22. Schuster DJ, Dykstra JA, Riedl MS, Kitto KF, Belur LR, McIvor RS, Elde RP, Fairbanks CA, Vulchanova L. Biodistribution of adeno-associated virus serotype 9 (AAV9) vector after intrathecal and intravenous delivery in mouse. Front Neuroanat. 2014;8:42. doi: 10.3389/fnana.2014.00042. [PubMed: 24959122]
23. Klein CJ, Duan X, Shy ME. Inherited neuropathies: clinical overview and update. Muscle Nerve. 2013;48(4):604–22. doi: 10.1002/mus.23775. [PubMed: 23801417]
24. Wang Z, Ma HI, Li J, Sun L, Zhang J, Xiao X. Rapid and highly efficient transduction by double-stranded adeno-associated virus vectors in vitro and in vivo. Gene Ther. 2003;10(26):2105–11. doi: 10.1038/sj.gt.3302133. [PubMed: 14625564]
25. Ohno K, Samaranch L, Hadaczek P, Bringas JR, Allen PC, Sudhakar V, Stockinger DE, Snieckus C, Campagna MV, San Sebastian W, Naidoo J, Chen H, Forsayeth J, Salegio EA, Hwa GGC, Bankiewicz KS. Kinetics and MR-Based Monitoring of AAV9 Vector Delivery into Cerebrospinal Fluid of Nonhuman Primates. Mol Ther Methods Clin Dev. 2019;13:47–54. doi: 10.1016/j.omtm.2018.12.001. [PubMed: 30666308]
26. Samaranch L, Sebastian WS, Kells AP, Salegio EA, Heller G, Bringas JR, Pivirotto P, DeArmond S, Forsayeth J, Bankiewicz KS. AAV9-mediated expression of a non-self protein in nonhuman primate central nervous system triggers widespread neuroinflammation driven by antigen-presenting cell transduction. Mol Ther. 2014;22(2):329–37. doi: 10.1038/mt.2013.266. [PubMed: 24419081]
27. Timmerman V, Strickland AV, Zuchner S. Genetics of Charcot-Marie-Tooth (CMT) Disease within the Frame of the Human Genome Project Success. Genes (Basel). 2014;5(1):13–32. [PubMed: 24705285]
28. Saporta MA, Shy ME. Inherited peripheral neuropathies. Neurol Clin. 2013;31(2):597–619. [PubMed: 23642725]
29. Morelli KH, Griffin LB, Pyne NK, Wallace LM, Fowler AM, Oprescu SN, Takase R, Wei N, Meyer-Schuman R, Mellacheruvu D, Kitzman JO, Kocen SG, Hines TJ, Spaulding EL, Lupski JR, Nesvizhskii A, Mancias P, Butler IJ, Yang XL, Hou YM, Antonellis A, Harper SQ, Burgess RW. Allele-specific RNA interference prevents neuropathy in Charcot-Marie-Tooth disease type 2D mouse models. J Clin Invest. 2019;129(12):5568–83. doi: 10.1172/JCI130600. [PubMed: 31557132]
30. Clement N, Grieger JC. Manufacturing of recombinant adeno-associated viral vectors for clinical trials. Mol Ther Methods Clin Dev. 2016;3:16002. doi: 10.1038/mtm.2016.2. [PubMed: 27014711]
31. Gray SJ, Choi VW, Asokan A, Haberman RA, McCown TJ, Samulski RJ. Production of recombinant adeno-associated viral vectors and use in in vitro and in vivo administration. Curr Protoc Neurosci. 2011;Chapter 4:Unit 4 17. doi: 10.1002/0471142301.ns0417s57.
32. Karumuthil-Melethil S, Nagabhushan Kalburgi S, Thompson P, Tropak M, Kaytor MD, Keimel JG, Mark BL, Mahuran D, Walia JS, Gray SJ. Novel Vector Design and Hexosaminidase Variant Enabling Self-Complementary Adeno-Associated Virus for the Treatment of Tay-Sachs Disease. Hum Gene Ther. 2016;27(7):509–21. doi: 10.1089/hum.2016.013. [PubMed: 27197548]

Highlights

- Intrathecal delivery of AAV9 in mice is highest near the site of injection and tapers as it spreads.
- Intrathecal delivery of AAV9 transduces peripheral nerves and autonomic nervous tissue, including sympathetic and enteric neurons.
- In the brain, AAV9/GFP vector spread and transduction is notably higher in brain regions near the site of injection following intracisternal delivery as compared to lumbar puncture delivery.
- In the lumbar spinal cord and peripheral organs, AAV9/GFP vector has higher distribution in LP-injected mice versus ICM-injected mice.
- Intracisternal or lumbar puncture intrathecal delivery of AAV9 efficiently transduces the CNS and to a lesser extent transduces the PNS and can be used to treat inherited neuropathies.

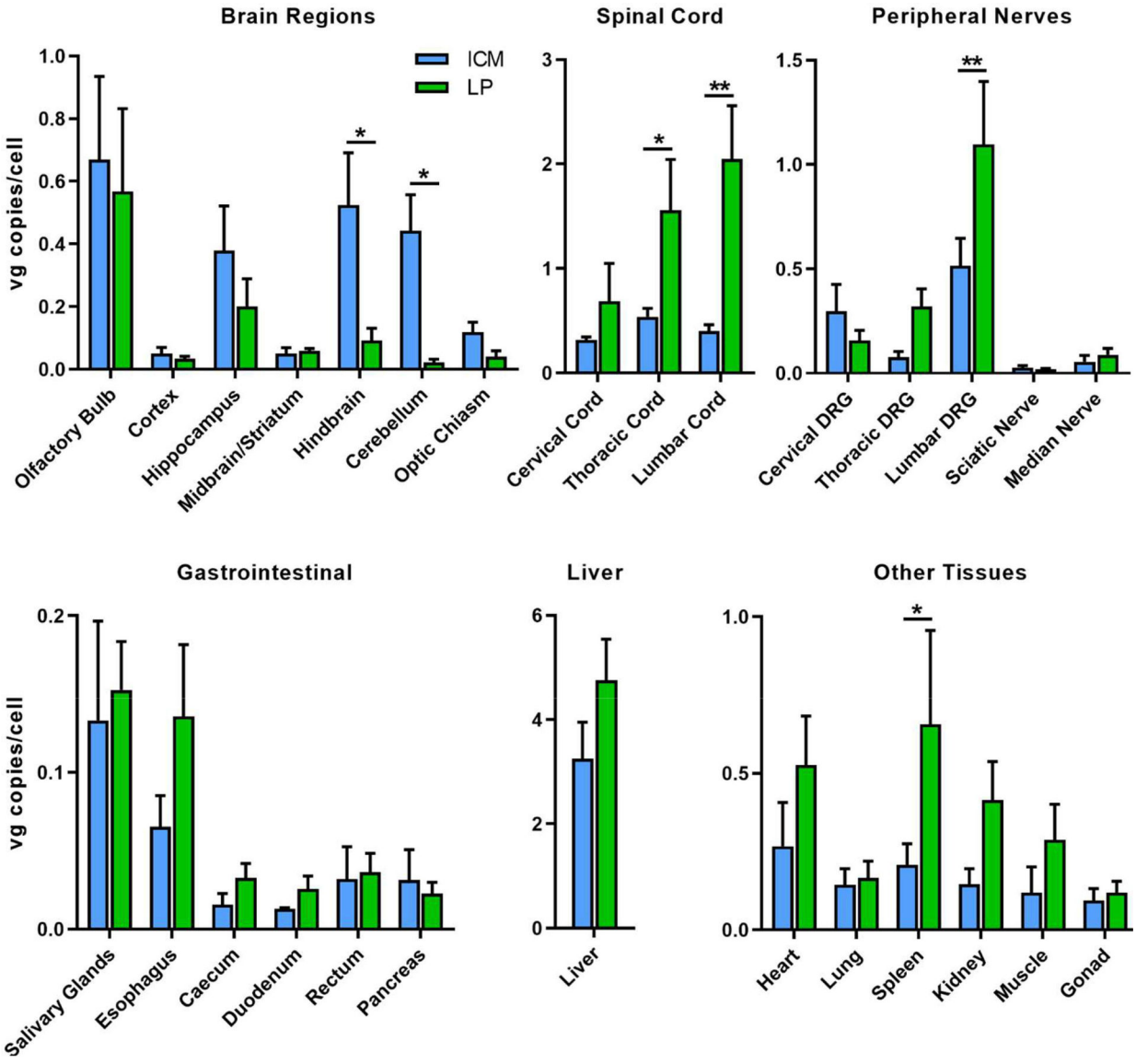

Figure 1.

Biodistribution of AAV9/GFP following intrathecal delivery in mice. AAV9 was administered to C57BL/6 mice at a dose of 4.15×10^{11} vg by injection into the cisterna magna (ICM) or the lumbar subarachnoid space (LP). All animals were sacrificed 4 weeks post-injection and vector genomes were quantified in tissue samples by qPCR. Vg copies are normalized to mouse lamin B as an endogenous housekeeping gene and are represented as vg copies per cell. Error bars represent SEM (n=4 per group). Each tissue group was analyzed by an unpaired t test. *p<0.5, **p<0.01. DRG, dorsal root ganglia.

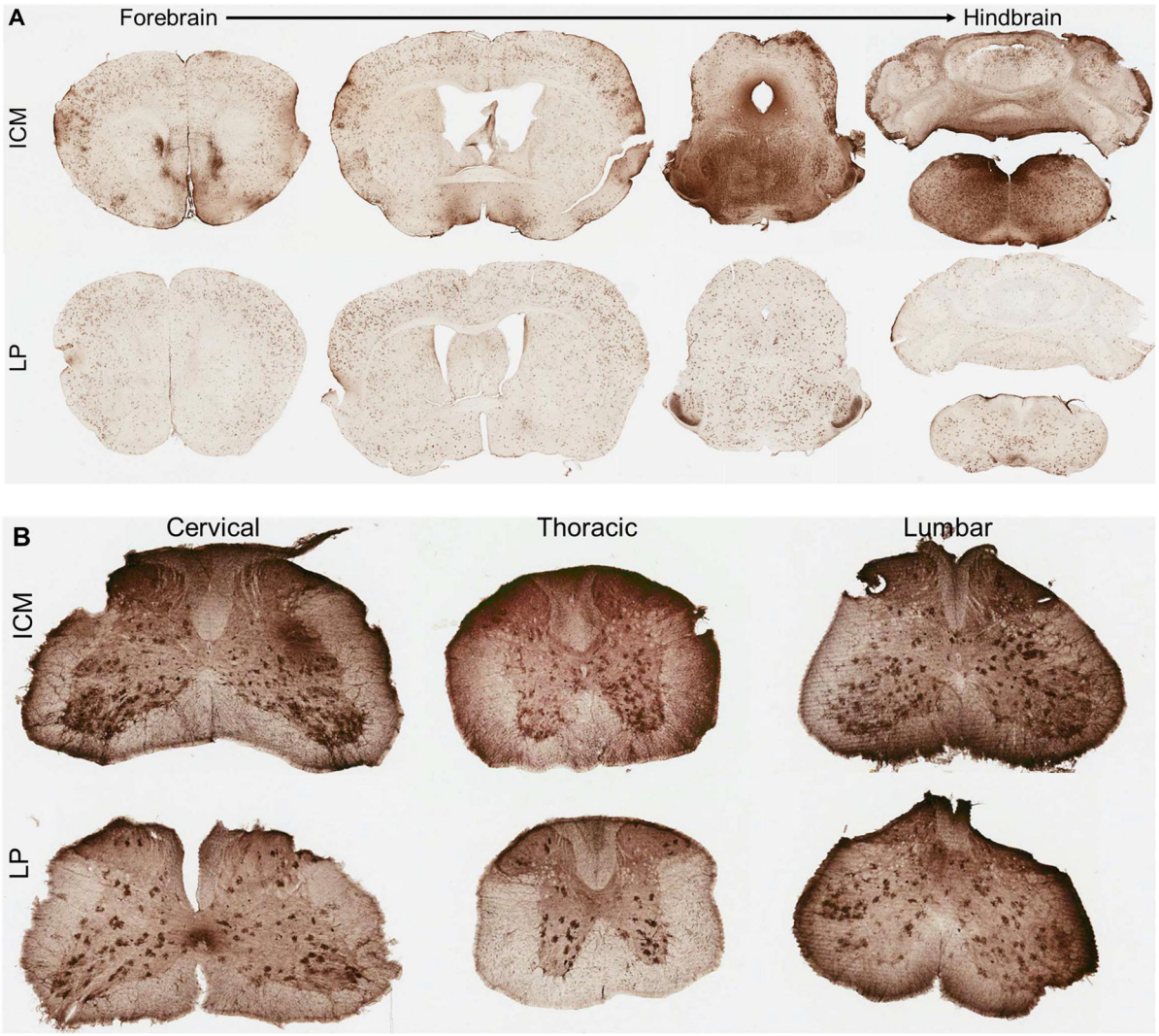

Figure 2.

CNS transduction profile of AAV9 following intrathecal delivery in mice. (A, B) Transduction profiles 4 weeks after intrathecal delivery of AAV9 packaging a scCBh-GFP transgene at a dose of 4.15×10^{11} vg via injection into the cisterna magna (ICM, top) or lumbar subarachnoid (LP, bottom) spaces across the (A) brain and (B) spinal cord. (A) Representative coronal sections from the whole mouse brain progressing from forebrain to the hindbrain (left to right). (B) Spinal cord sections from cervical (left), thoracic (middle) and lumbar (right) regions.

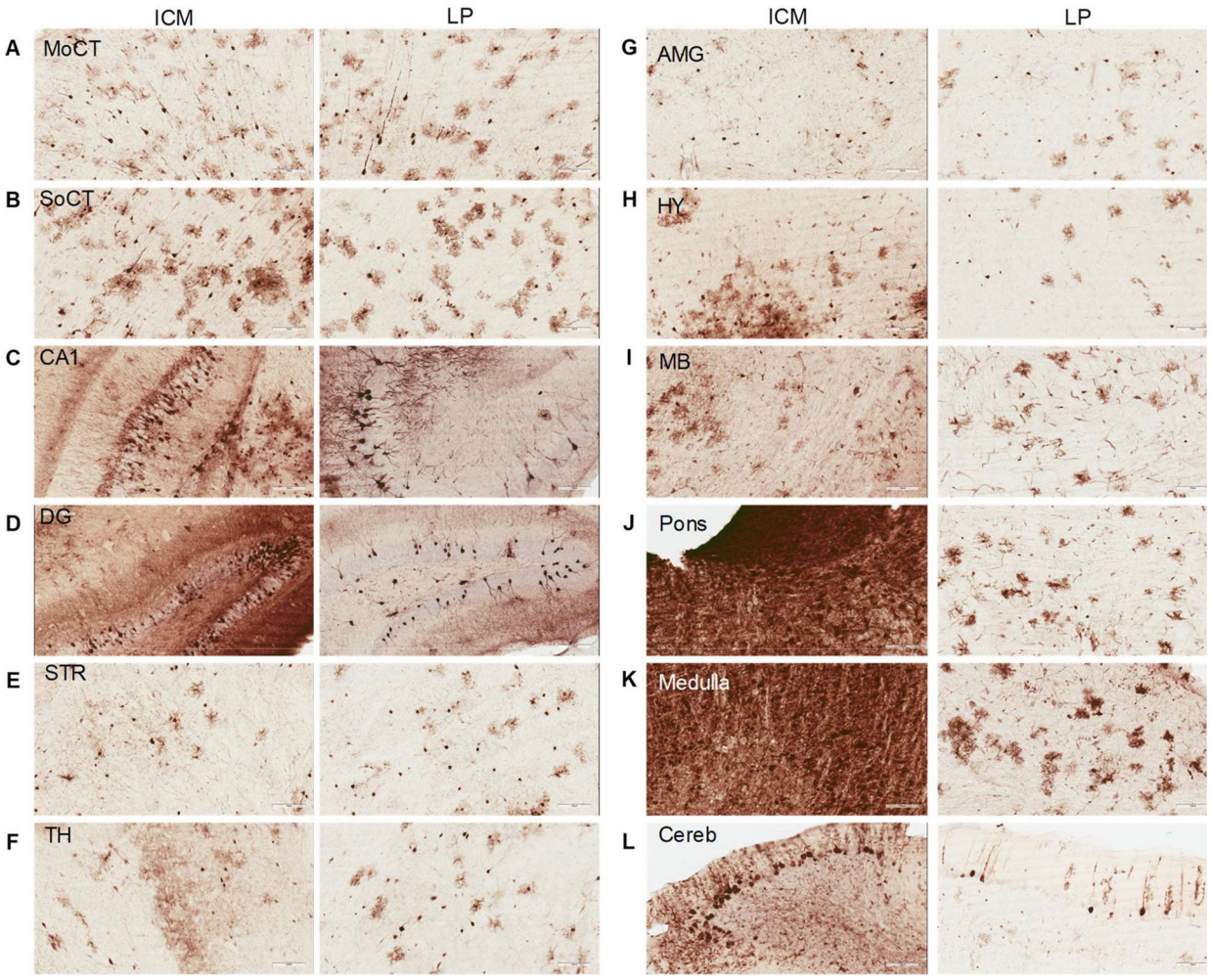

Figure 3.

Transduction throughout the brain following ICM and LP AAV9 delivery. (A-L) Expression profile 4 weeks after intrathecal delivery of scAA9/CBh-GFP vector at a dose of 4.15×10^{11} vg. (A) motor cortex, (B) somatosensory cortex, (C) CA1 of hippocampus, (D) dentate gyrus of hippocampus, (E) striatum, (F) thalamus, (G) amygdala, (H) hypothalamus, (I) midbrain, (J) pons, (K) medulla, and (L) cerebellum. Scale bars, 100 μm.

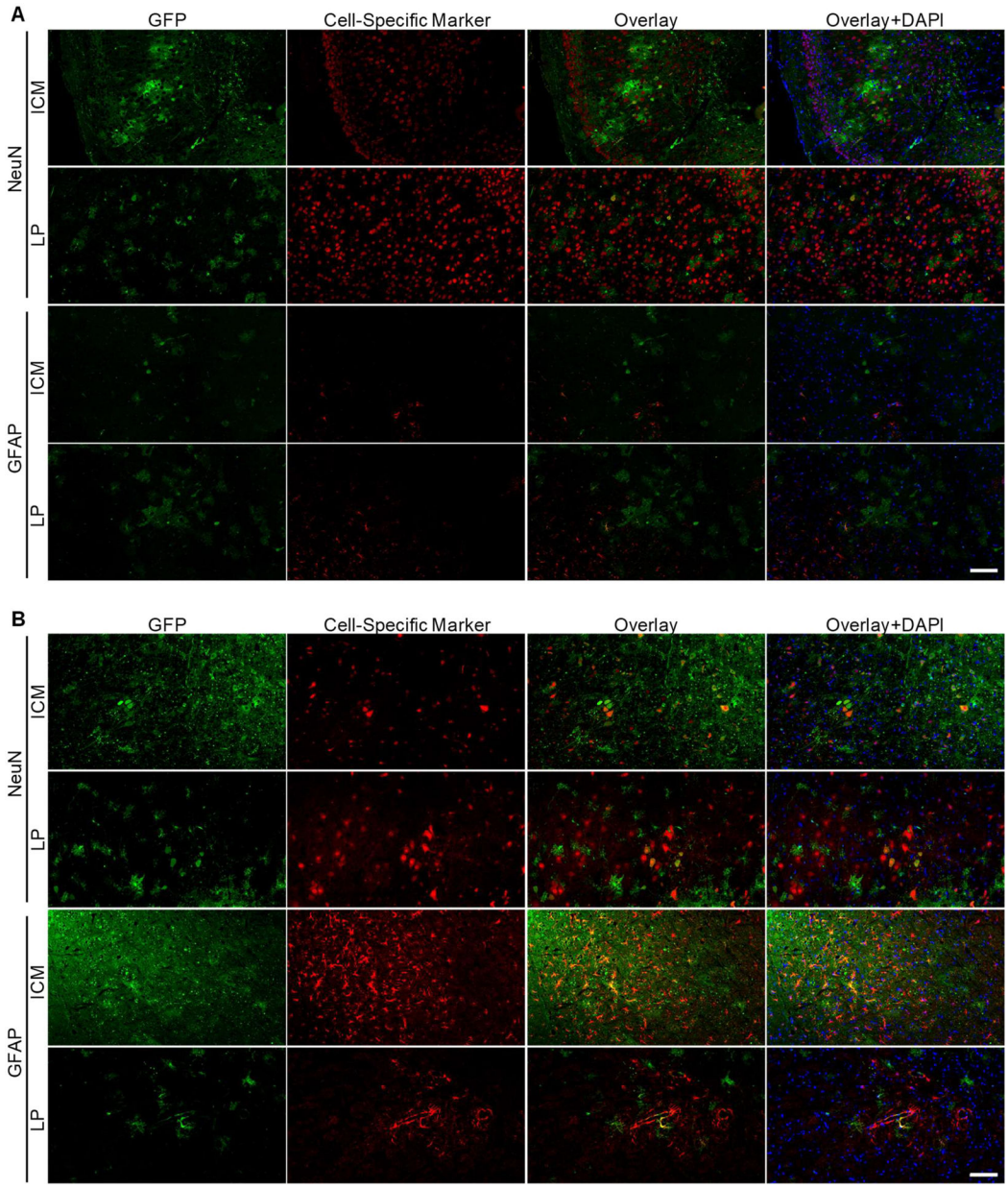

Figure 4.

Intrathecal AAV9 transduces neurons and glia in mice. (A) Cortical brain sections and (B) medulla brain sections from mice injected by ICM or LP routes were imaged for GFP expression. Sections are 5 μm thick. Images were overlaid with NeuN immunostaining for neurons or GFAP immunostaining for astrocytes. Counterstain is DAPI. Scale bar = 100 μm.

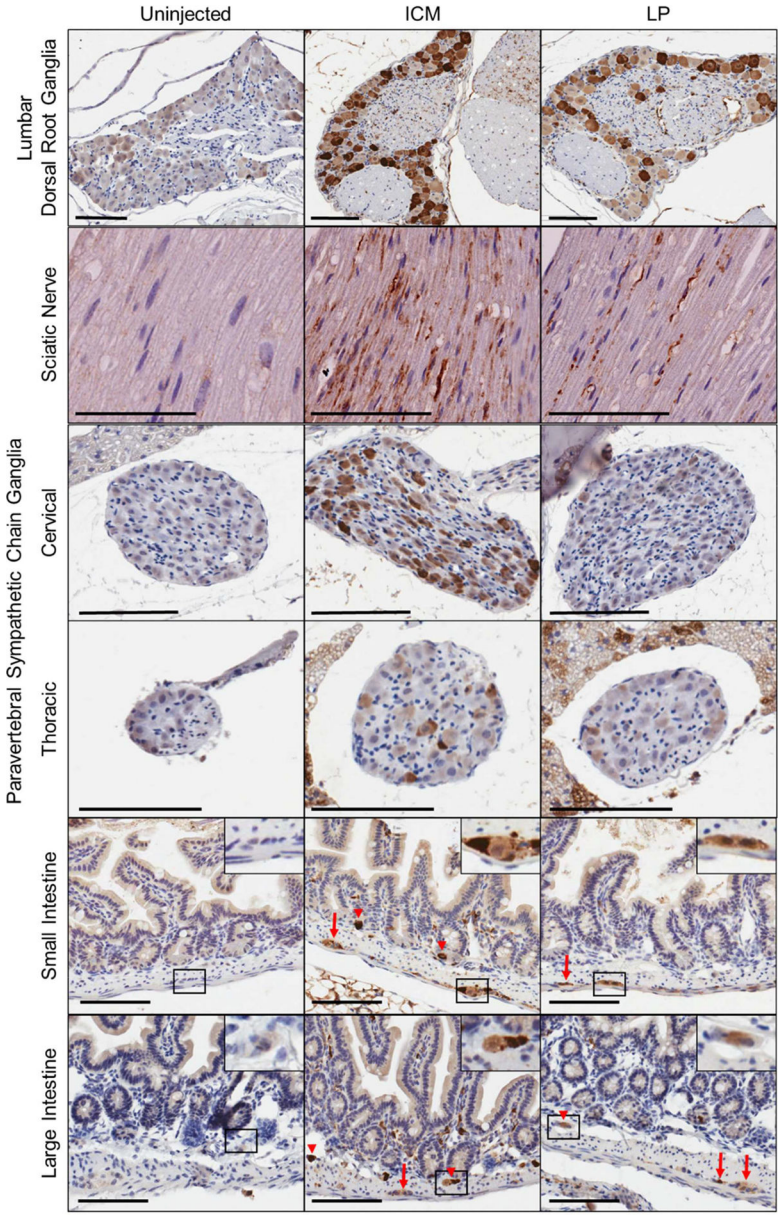

Figure 5.

Intrathecal delivery of scAAV9 vector results in peripheral nervous system expression. Tissues were collected 4 weeks after ICM or LP delivery of scAA9/CBh-GFP vector at a dose of 4.15×10^{11} vg in mice. Sections are 5 μm thick, stained with anti-GFP and counterstained with hematoxylin. Arrows, Myenteric plexus; arrow heads, submucosal plexus. Scale bars, 100 μm.